ChemPubSoc Europe

DOI: 10.1002/chem.201604206

CHEMISTRY A European Journal Full Paper

NMR Spectroscopy

Optimal Bicelle Size *q* for Solution NMR Studies of the Protein Transmembrane Partition

Alessandro Piai[+], Qingshan Fu[+], Jyoti Dev, and James J. Chou*[a]

Abstract: Structural characterization of transmembrane proteins in isotropic bicelles has become an increasingly popular application of solution NMR spectroscopy, as the fast-tumbling bicelles are membrane-like, yet can often yield spectral quality comparable to those of detergent micelles. While larger bicelles are closer to the true lipid bilayer, it remains unclear how large the bicelles need to be to allow accurate assessment of the protein transmembrane partition in the lipid bilayer. Here, we address the above question from the perspective of the protein residing in the bicelles, through systematic measurement of the protein chemical shift and transmembrane partition at different lipid/detergent ratios (*q*), ranging from 0.3 to 0.7, using the transmembrane domain of the human Fas receptor as model system. We found that the lipid environment of the bicelles, as reflected by the protein chemical shift, begins to be perturbed when *q* is reduced to below 0.6. We also implemented a solvent paramagnetic relaxation enhancement (PRE) approach for bicelles to show that the protein transmembrane partition in bicelles with $q=0.5$ and 0.7 are very similar, but at $q=0.3$ the solvent PRE profile is significantly different. Our data indicate that *q* values between 0.5 and 0.6 are a good compromise between high resolution NMR and closeness to the membrane environment, and allow accurate characterization of the protein position in the lipid bilayer.

Introduction

Transmembrane domains (TMDs) of many cell-surface receptors are not merely inert single-helix anchors; their oligomerization often plays essential roles in receptor assembly in the membrane and receptor signaling across the membrane. The modes of association between the transmembrane (TM) helices directly link the conformational state of the extracellular receptor domain to that of the intracellular signaling domains, thus modulating the transmission of signals across the membrane.[1] The membrane-associated regions of TM receptors have historically been very difficult to crystalize, except for a few very recent breakthroughs,[2] and they are also too small for the state-of-the-art cryo-electron microscopy technology. For these reasons, solution NMR has been frequently used for deriving high resolution structural information for these small and hydrophobic systems.[3] The combination of bicelles and solution NMR is particularly attractive, because bicelles have the potential to offer an essentially lipid bilayer environment, while concurrently being compatible with high resolution NMR spectroscopy that enables de novo structure determination of TM proteins.

Bicelles are composed of long-chain phospholipids that form the lipid bilayer disc and detergents that enclose the exposed hydrophobic side of the disc, such that the aggregate is soluble and fast tumbling in water.[4] The lipids are commonly long-chain phospholipids such as dimyristoyl phosphatidylcholine (DMPC). As for detergents, dihexanoyl phosphatidylcholine (DHPC), 3-(cholamido-propyl)dimethylammonio-2-hydroxy-1-propane-sulfonate (CHAPSO),[5] and 6-cyclohexyl-1-hexyl-phosphocholine (Cyclofos-6)[6] have been shown to be compatible with the bicelle formation, among which DHPC is by far the most used in structural studies of TM proteins. In an ideal bicelle (lipid and detergent well segregated), the size of the bicelle can be estimated based purely on geometric arguments,[7] i.e., the radius of the bilayer region of the bicelle (*R*) can be calculated directly from the lipid/detergent molar ratio (*q*).[8]

While it is generally agreed upon that larger *q* values yield more ideal bicelles, it remains vague how large the *q* needs to be to provide a planar bilayer environment for the proteins residing within. For solution NMR studies, smaller bicelles are obviously preferred, and essentially all successful bicelle applications in solving atomic resolution structures of TMDs have been achieved using bicelles with $q \leq 0.5$.[1c,3f,9] In those earlier studies, however, bicelles were used mainly as an effective solubilization system of membrane proteins, and the potential of bicelles in providing information about protein partition in the lipid bilayer, which is an important aspect of the TMD structure, has not been fully exploited. In this study, we use the homo-trimeric TMD of the human Fas receptor as a model system to identify the optimal bicelle size that compromises

[a] Dr. A. Piai,[+] Dr. Q. Fu,[+] J. Dev, Dr. J. J. Chou
Department of Biological Chemistry and Molecular Pharmacology
Harvard Medical School
Boston, Massachusetts 02115 (USA)
E-mail: james_chou@hms.harvard.edu

[+] These authors contributed equally.

Supporting information and ORCID number(s) for the author(s) of this article can be found under http://dx.doi.org/10.1002/chem.201604206.

high resolution NMR and the ability to allow accurate assessment of protein TM partition in a lipid bilayer.

Results and Discussion

Fas is an apoptosis-inducing death receptor in the tumor necrosis factor receptor superfamily,[10] and its TMD structure was previously determined by solution NMR in DMPC/DHPC bicelles.[1c] The structure shows that the TM helices pack around a proline-containing sequence motif to form a homotrimer with C3 symmetry. We first examined the effect of bicelle q on the Fas TMD NMR spectrum using the "q-titration" method,[11] because the chemical shift is exquisitely sensitive to the surrounding surfactant environment, especially when the bicelle changes from lipid-disk-like (lipids and detergents segregated) to mixed-micelle-like (lipids and detergents mixed). We began with the Fas TMD reconstituted in DMPC/DHPC bicelles with $q=0.7$ and monitored the spectral changes as we gradually reduced the q to 0.3 by titrating the sample with DHPC. The 2D ^{1}H-^{15}N TROSY-HSQC spectrum of the Fas TMD essentially did not change when reducing the q from 0.7 to 0.6, but further reducing the q to 0.5 and below caused substantial changes in chemical shifts (Figure 1 and Figure S1 in the Supporting Information). Residues in the N- and C-termini (residues 173–175 and 193–195) exhibited the largest changes.

This result indicates that the lipid environments experienced by the TMD in bicelles with $q=0.7$ and 0.6 are essentially the same; it also implies that the DMPC and DHPC molecules are well segregated, as an increase in DHPC could not affect the protein that is exclusively associated with the lipid bilayer region of the bicelles. Conversely, the steady resonance shifts observed from $q=0.5$–0.3 suggest that in this q range the TMD chemical environment is more affected due to increasing mixing of DHPC into the DMPC bilayer region.

As independent validation of the increased bicelle size at larger q, the effective TMD rotational correlation time (τ_c) was measured using the TRACT method[12] (Figure S2 in the Supporting Information). We found that the apparent protein τ_c at 30 °C, as probed by the N-terminal residue, is 13, 20, and 32 ns for q values of 0.3, 0.5, and 0.7, respectively. These results explain why smaller bicelles are generally preferred for high-resolution NMR studies of TMDs. However, only ideal bicelles with a discoidal profile at higher q afford the opportunity to characterize the TMD transmembrane partition.

We, thus, examined the partition of the Fas TMD in bicelles with q values of 0.7, 0.5, and 0.3, to provide a guideline for the

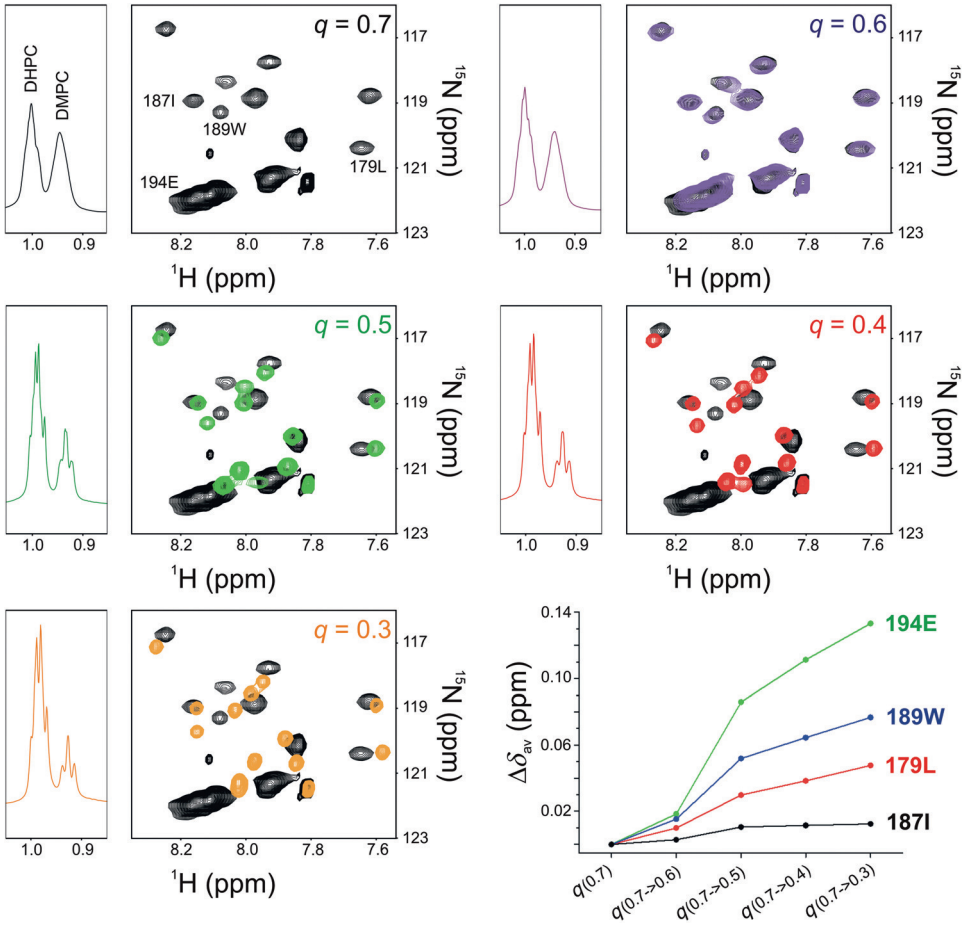

Figure 1. Chemical shift changes of Fas receptor TMD (transmembrane domain) induced by changing bicelle q. The central region of the 2D ^{1}H-^{15}N TROSY-HSQC spectrum is shown for $q=0.7$ (black), 0.6 (purple), 0.5 (green), 0.4 (red), and 0.3 (orange). On the left of each 2D spectrum, the methyl signals of DMPC (dimyristoyl phosphatidylcholine) and DHPC (dihexanoyl phosphatidylcholine) from the 1D ^{1}H spectrum are provided to indicate bicelle q. The bottom right plot shows chemical shift changes at various q values relative to $q=0.7$ for residues 179, 187, 189, and 194.

selection of the optimal q value for this type of application. Accurate determination of the protein partition in lipid bilayers remains a challenging task in structural biology. In solution NMR studies, measuring the nuclear Overhauser enhancement (NOE) between protein and lipid acyl chains and headgroups has been the most common method to address this problem.[13] This approach, however, can only provide a rather qualitative description of the lipid/detergent distribution around the protein due to the dynamic nature of the lipid and detergent molecules. Alternatively, paramagnetic agents such as Gd-DTPA-BMA, Gd-DOTA, O_2, and Mn^{2+} ions have been successfully used to probe membrane immersion depth of protein domains.[14] The majority of these studies, however, has been designed for detergent micelles and, thus, could not be employed for the purpose of our study. Therefore, we implemented a solvent paramagnetic relaxation enhancement (PRE) approach for bicelle applications to overcome the technical hurdle.

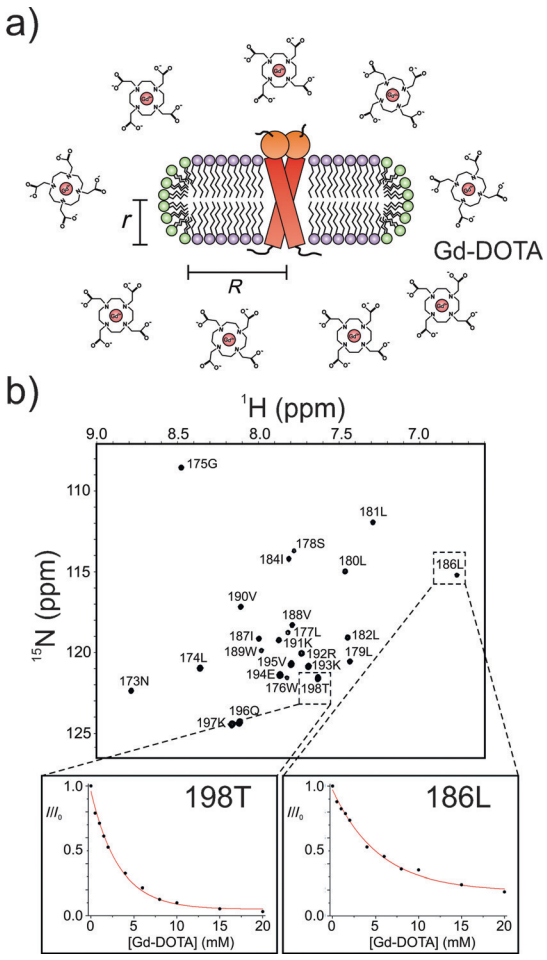

Figure 2. The paramagnetic-agent titration strategy for probing the membrane-immersion depth. a) Schematic illustration of titrating bicelle-reconstituted TMD with Gd-DOTA. R and r are the radii of the planar region and the rim, respectively. b) PREs (paramagnetic relaxation enhancements) induced by Gd-DOTA titration, measured in 2D ^{1}H-^{15}N TROSY-HSQC spectra of Fas TMD reconstituted in $q = 0.5$ bicelles. The PRE (or I/I_0, as defined in the text) versus the Gd-DOTA concentration is shown for residues 186 (buried) and 198 (exposed).

In this approach (schematically illustrated in Figure 2a), the TMD is reconstituted in bicelles and titration of paramagnetic agents outside the bicelles is performed to generate solvent paramagnetic fields of varying strength. The resulting residue-specific signal-reduction profiles due to the PRE are then analyzed collectively to determine the protein region that resides at the center of the bilayer. This method has a number of requirements for it to be of practical use: 1) The paramagnetic agent must be water soluble and bicelle inaccessible, so that the PRE it generates decreases with distance from the bicelle surface to the core, and by not having a membrane partition the paramagnetic molecule avoids potential non-specific interactions with the protein that could mislead the PRE interpretation. Paramagnetic agents such as Gd-DOTA and Gd-DTPA-BMA satisfy these requirements; 2) The role of the paramagnetic agent is to probe the protein-immersion depth along the bicelle normal (or longitudinal axis). Hence, the bicelles need to be sufficiently large to exclude lateral contributions from the surrounding paramagnetic field. This is critical, because for very small bicelles, e.g., lipid/detergent ratios (q) < 0.3, we would encounter the mixed micelle situation in which it is essentially impossible to deconvolute the longitudinal and lateral components of the solvent PRE.

A critical aspect of the experimental design was to perform a paramagnetic agent titration rather than a single addition, as a wide range of paramagnetic field strengths (from very weak to strong) are required to probe both solvent-exposed and buried protein regions. We titrated the bicelle-reconstituted Fas TMD with Gd-DOTA at a Gd-DOTA/TMD ratio of 1–40. At each of the titration points, a 2D ^{1}H-^{15}N TROSY-HSQC spectrum was recorded to measure the residue-specific PRE, defined here as I/I_0, in which I and I_0 are the intensities of a peak in the presence and absence of the paramagnetic agent, respectively. The NMR titration generated a PRE versus Gd-DOTA concentration profile (Figure 2b) for each of the assigned residues of the TMD, which could be described by the following exponential decay [Eq. (1)][14b]:

$$\frac{I}{I_0} = 1 - \mathrm{PRE}_{\mathrm{amp}}\left(1 - e^{-\frac{[\text{Gd-DOTA}]}{\tau}}\right) \quad (1)$$

in which I and I_0 are as defined above, [Gd-DOTA] is the concentration of the paramagnetic agent, τ is the decay constant, and $\mathrm{PRE}_{\mathrm{amp}}$ is the amplitude of the PRE that can be experienced by each of the reporting nuclear spins in the protein. In this study, we chose backbone amide protons as the dominant PRE reporters. Fitting the I/I_0 versus the [Gd-DOTA] data points according to Equation (1) yielded a residue-specific $\mathrm{PRE}_{\mathrm{amp}}$ (Figure 2b and Table S2 in the Supporting Information). The complete $\mathrm{PRE}_{\mathrm{amp}}$ versus residue number plot is shown in Figure 3a.

In previous studies of solvent PREs, it was shown for water-soluble proteins that, if the protein structure is known, the $\mathrm{PRE}_{\mathrm{amp}}$ for each of the ^{1}H in the protein can be predicted by integrating the PRE between the ^{1}H and an infinitesmal volume outside surrounding the protein structure (with the r^{-6} distance dependence) over a defined cube in which the protein structure resides.[15] This PRE calculation, however, would be extremely difficult to implement for a bicelle-reconstituted pro-

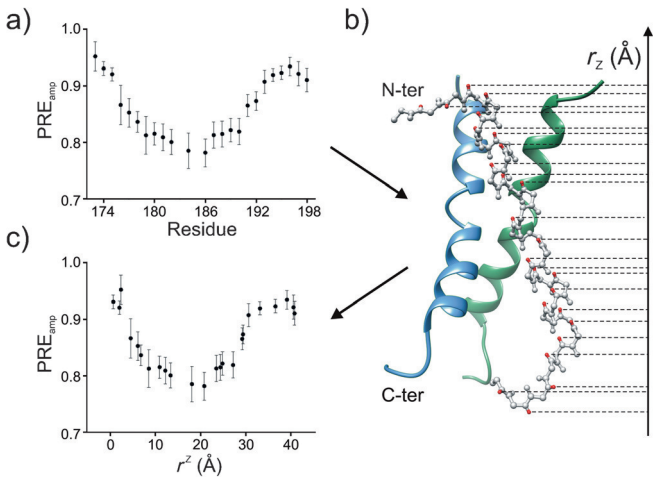

Figure 3. Residue-specific PRE_{amp} and position-specific PRE_{amp}. a) PRE_{amp} versus residue number for the Fas TMD reconstituted in $q=0.5$ bicelles. b) The NMR structure of the Fas TMD homotrimer with the symmetry axis aligned with the bicelle normal, showing the amide protons (red spheres) for which PRE_{amp} has been determined. The dashed lines point to the projected positions (r_z) of the amide protons onto the C3 axis. c) PRE_{amp} versus r_z plot. The r_z reference point is arbitrarily chosen, e.g., $r_z=0$ for the N-terminus.

tein due to the added unknowns about the protein position relative to the bicelle, as well as the potentially dynamic morphology of the fast tumbling bicelles.

For these reasons, we preferred a simple mathematical fitting approach to analyze the PRE_{amp} data with the practical goal of determining the distance between each TMD residue and the center of the lipid bilayer of the bicelle. To convert PRE_{amp} versus residue number (Figure 3a) to PRE_{amp} versus bilayer immersion depth, we calculated, for each residue *i*, the distance along the bilayer normal (r_z) from the amide proton to an arbitrary reference point based on the protein structure. Since the Fas TMD is a homotrimer, its symmetry axis is parallel to the bilayer normal, which allowed a convenient calculation of r_z (Figure 3b and Figure S3 in the Supporting Information). The PRE_{amp} versus r_z plot shows a sigmoidal profile (Figure 3c). We, thus, fitted the PRE_{amp} versus r_z data with the symmetric sigmoid equation, which has been used previously to approximate the O_2 concentration gradient across a lipid bilayer.[14d,16] Here, the equation has been implemented to describe PRE_{amp} as a function of $|r_z|$ [Eq. (2)]:

$$PRE_{amp} = PRE_{amp}^{min} + \frac{\left(PRE_{amp}^{max} - PRE_{amp}^{min}\right)}{1 + e^{(r_z^I - |r_z|)/SLOPE}} \quad (2)$$

in which PRE_{amp}^{min} and PRE_{amp}^{max} are the limits within which PRE_{amp} can vary for a particular protein system, r_z^I is the inflection point (the distance from the bilayer center at which PRE_{amp} is halfway between PRE_{amp}^{min} and PRE_{amp}^{max}), and SLOPE is a parameter which reports the steepness of the curve at the inflection point. Equation (2) empirically describes three PRE regimes: the PRE-saturated regime near the bicelle surface and the PRE-insensitive regime in the lipid core, connected by the PRE-sensitive regime that shows the r^{-6} dependence to the first-order approximation. Moreover, by the symmetry assumption of the fast-tumbling bicelles, the bilayer center should lie at the middle of the bottom flat region of Equation (2). This means that, if the bilayer center is correctly assigned to the protein, the PRE data should fit very well to this symmetric function.

Based on the above rationale, we systematically slid the Fas TMD along the bicelle normal relative to the bilayer center to achieve a best fit to Equation (2), as illustrated in Figure 4a and Figure S4 in the Supporting Information. At each TMD position, the adjusted coefficient of determination (R^2_{adj}) was obtained, as shown in Figure 4b in the case of $q=0.5$. The TMD position that yielded the highest R^2_{adj} was assigned as the protein position in the bilayer region of the bicelles (Figure 4c, Figure S5 and Table S3 in the Supporting Information).

The above solvent PRE measurement and analysis were performed for bicelles with q values of 0.3, 0.5, and 0.7 (residue-specific PRE_{amp} shown in Figure S6). For $q=0.7$, data fitting shows that the Ile184 amide proton lies almost exactly at the middle of the bilayer (Figure 5a). The bilayer center derived from the $q=0.5$ bicelle is only slightly shifted by 0.9 Å compared to the results from the $q=0.7$ bicelle. For $q=0.3$, however, the PRE_{amp} versus r_z profile is drastically different from that of $q=0.5$ or 0.7 bicelles, and the bilayer center from data fitting is shifted by 2.5 Å compared to that of the $q=0.7$ bicelle.

The different results obtained for the tested q values can be explained by the following arguments. The analysis of solvent PRE using the sigmoidal function is based on the premise that the bicelle has a sufficiently large planar bilayer region to exclude most, if not all, of the lateral solvent PRE, such that the longitudinal PRE is the dominant factor in probing the TMD immersion depth. In the case of the bicelle with $q=0.7$, the theoretical bilayer radius R is roughly 30.4 Å (or $R+r\approx 50$ Å),[8] which should in principle eliminate a lateral paramagnetic effect. The position of the human Fas TMD in the bilayer region of the bicelle, as derived from the $q=0.7$ bicelle, should, thus, provide an accurate picture of the Fas TMD in the context of the lipid bilayer. The TM helices are completely immersed in the lipid bilayer (Figure 5b). The critical Pro185 sidechain important for the trimer assembly is almost exactly at the center of the bilayer.

The result that bicelles with $q=0.7$ and 0.5 yielded very similar sigmoidal profiles and positions with respect to the bilayer center indicates that both bicelles have defined discoidal shapes. On the contrary, the very different sigmoidal profile of the bicelle with $q=0.3$ suggests that the shape of this bicelle deviates significantly from that of an ideal bicelle and is more mixed-micelle-like. Notably, the PRE-saturated regime region at $q=0.3$ reported in Figure 5a shows a significant upward shift relative to those at $q=0.5$ and 0.7. This can be explained by a larger lateral paramagnetic effect on the N- and C-terminal ends of the TMD near the bicelle surface. As for the comparison between $q=0.5$ and $q=0.7$, the PRE-saturated regimes are the same, although the PRE-insensitive regime at $q=0.5$ shows a larger PRE_{amp} than that at $q=0.7$. This observation can be explained by the fact that, for the protein terminal regions

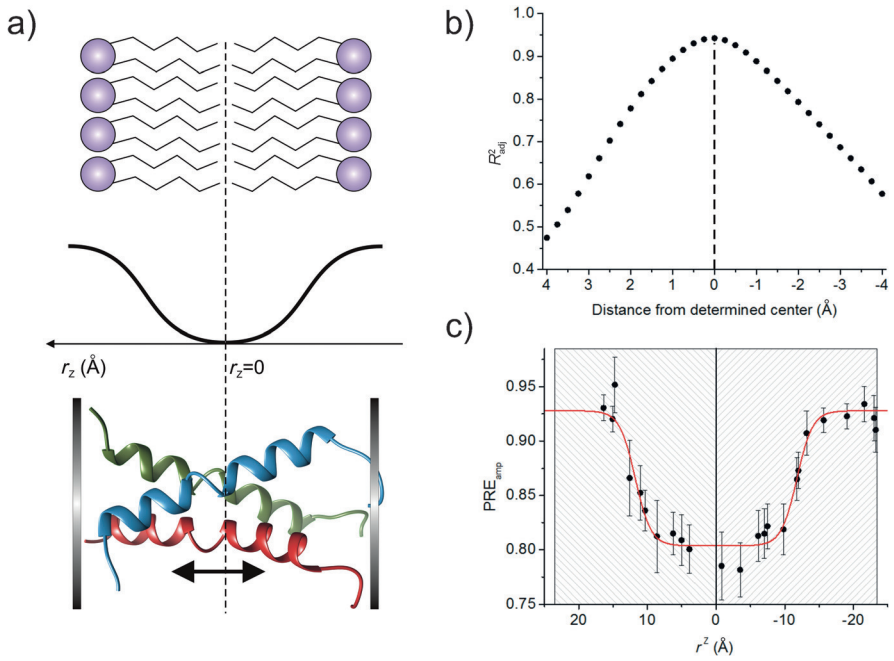

Figure 4. Assignment of the bilayer center to the Fas TMD by data fitting. a) Schematic illustration of the symmetric sigmoidal profile used to describe PRE$_{amp}$ along the bilayer normal (r_z). The protein is translated along the bilayer normal to generate PRE$_{amp}$ versus r_z data that best fit the sigmoidal function. b) The adjusted coefficient of determination (R^2_{adj}) from data fitting versus deviation of the true bilayer center. The data is from $q=0.5$ bicelles. The plot shows that R^2_{adj} is a reliable indicator of the protein position with an error of about ± 0.5 Å. c) The optimized fit of the PRE$_{amp}$ versus r_z data to Equation (2) from (b). The gray-striped box represents the thickness of the DMPC bilayer (considering both hydrocarbon and headgroup regions)[17].

near the bicelle surface, the longitudinal component of the PRE dominates over the lateral component, and, thus, no significant changes are observed; conversely, in the bilayer core in which the longitudinal component of the PRE is weak, the small increase in the lateral PRE at $q=0.5$ is no longer negligible, resulting in the upward shift of the PRE-insensitive regime.

Conclusion

In conclusion, we have shown, from the perspective of a bicelle-reconstituted TMD, that DMPC/DHPC bicelles with $q \geq 0.6$ provide the same phospholipid environment for the protein as indicated by NMR chemical shifts, and that this environment is very close to the planar lipid bilayer as shown by our solvent PRE analysis. Although protein chemical shifts at $q=0.5$ show small differences relative to those at $q=0.6$ and 0.7, the overall TM partition of the protein is essentially the same, suggesting that bicelles with $q=0.5$ are still very close to ideal bicelles. This conclusion obtained from the perspective of bicelle-reconstituted protein is consistent with earlier biophysical studies of empty bicelles,[8] which showed that DMPC/DHPC bicelles with $q=0.5$ adopt a discoidal shape. In consideration of the significantly better Fas TMD τ_c at $q=0.5$ (20 ns at 30 °C) compared to that at $q=0.7$ (32 ns), we propose that q values between 0.5 and 0.6 should be a good compromise between high resolution liquid-state NMR and closeness to the lipid bilayer environment. We, thus, recommend using bicelles of this q values to obtain a TM partition of membrane-embedded protein domains. Finally, the above conclusion is based on results derived for DMPC/DHPC bicelles at 30 °C, which represents one of the most common conditions for solution NMR studies of TMDs. Since melting temperatures of frequently used bicelle lipids, such as DMPC, POPC, and POPG, are well below 30 °C,[17–18] the temperature effect on our analysis should be negligible if it is above the lipid phase transition temperature. The general analysis method reported here should also apply to bicelle detergents different from DHPC, though the optimized q may differ slightly[19] and thus, requires experimental validation.

Experimental Section

Protein expression, purification, and reconstitution: The (^{15}N, ^{2}H)-labeled human Fas TMD was expressed and purified as previously described.[1c] The lyophilized protein (1–2 mg) was dissolved in hexafluoroisopropanol (HFIP) with approximately 9 mg DMPC, followed by drying of the solution under a nitrogen stream to achieve a thin film. The thin film was then dissolved in 3 mL of an 8 M urea solution containing approximately 27 mg DHPC, followed by dialysis against 20 mM sodium phosphate buffer at pH 6.8 to remove the denaturant. After dialysis, DHPC was added to adjust the ratio of DMPC/DHPC (q) to the desired value. The solution with reconstituted Fas TMD was concentrated using a centricon to prepare the final NMR sample containing 500 μM Fas TMD, 60 mM DMPC, and 200, 120, or 85 mM DHPC (for $q=0.3$, 0.5, or 0.7, respectively) and 20 mM sodium phosphate (pH 6.8). 10% (v/v) D_2O was added for the NMR lock. The final DMPC/DHPC ratio of the samples was determined by integrating the resolved methyl peaks of DMPC and DHPC in the 1D ^{1}H NMR spectra.

DHPC titration: The Fas TMD was reconstituted in $q=0.7$ bicelles and DHPC was progressively added to reduce the bicelle size. The

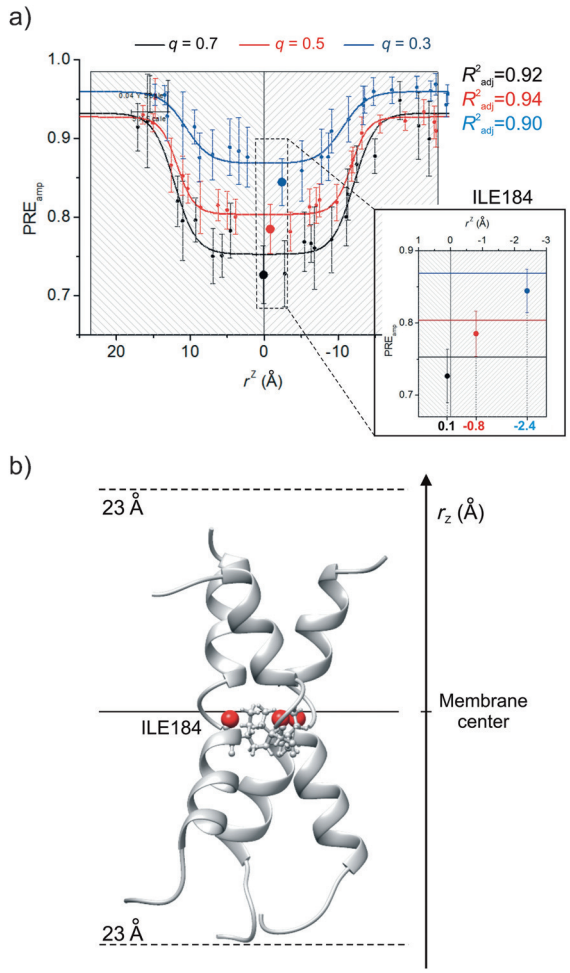

Figure 5. Fas TMD transmembrane partition analysis at different bicelle *q*. a) Comparison of PRE_{amp} versus r_z data fitting from the $q=0.7$ (black), 0.5 (red), and 0.3 (blue) bicelles. In the zoomed region, the r_z distance of Ile184 from the bilayer center ($r_z=0$) is shown. b) Position of the Fas TMD in the lipid bilayer. The solid and dashed lines represent the center and the boundaries of the DMPC bilayer, respectively. The Ile184 $^1H^N$ is shown as red sphere.

detergent was taken from a concentrated stock solution (660 mM DHPC) made in the same buffer of the protein sample and it was added in small aliquots (few µL per step) to minimize possible dilution effects. To monitor the progress of the titration by NMR, a 2D ^1H-^{15}N TROSY-HSQC spectrum was recorded at 600 MHz (Table S1) at each of the following *q* values: 0.7, 0.6, 0.5, 0.4, and 0.3. The chemical shift assignments of the human Fas TMD was taken from the Biological Magnetic Resonance Bank (BMRB),[20] entry 25930[1c].

τ_c Determination: The Fas TMD was reconstituted in $q=0.7$, 0.5, and 0.3 bicelles. For each *q*, a series of 1D ^1H-^{15}N TRACT spectra was recorded at 600 MHz (Table S1) with the following relaxation time: 4, 12, 20, 28, 36, 44, 52, 64, 76, and 100 ms. For each time point, the TROSY and anti-TROSY signals were acquired separately.

Gd-DOTA titrations: The Fas TMD was reconstituted in $q=0.7$, 0.5, and 0.3 bicelles and titrated against a known concentration of Gd-DOTA. The titrant was taken from a concentrated stock solution (600 mM Gd-DOTA) in the same buffer as that of the protein sample, and it was added in small aliquots (few µL per step) to minimize possible dilution effects. To monitor the progress of the titration by NMR, a 2D ^1H-^{15}N TROSY-HSQC spectrum was recorded at 600 MHz (Table S1) at each of the following titrant concentrations: 0.5, 1.0, 1.5, 2.0, 4.0, 6.0, 8.0, 10.0, 15.0, and 20.0 mM.

NMR data acquisition, processing, and analysis: The NMR experiments were performed at 14.1 T on a Bruker Avance III HD spectrometer operating at 600.13 MHz (^1H), 150.90 MHz (^{13}C), and 60.81 MHz (^{15}N) frequencies and on a Bruker Avance I spectrometer operating at 600.47 MHz (^1H), 150.99 MHz (^{13}C), and 60.85 MHz (^{15}N) frequencies, both equipped with a cryogenically cooled probe head. All the measurements were performed at 303.0 K. The most relevant acquisition parameters of the experiments are reported in Table S1. The NMR data sets were processed using NMRPipe[21] and the resulting NMR spectra were analyzed with Sparky (T. D. Goddard and D. G. Kneller, SPARKY 3, University of California, San Francisco). Topspin was used to measure integrals in 1D spectra. Chemical shift variations were quantified using the formula $\Delta\delta = \sqrt{\Delta\delta_{HN}^2 + (\Delta\delta_N/5)^2/2}$. Peak intensities were measured at the peak local maximum using quadratic interpolation to identify the peak center. Origin (OriginLab, Northampton, MA) was used to fit the experimental data.

Derivation of Equation 1: The general form of the exponential decay reported in Equation (1) is:

$$\frac{I}{I_0} = \lim_{[Gd-DOTA]\to\infty}\left(\frac{I}{I_0}\right) + PRE_{amp}\, e^{-[Gd-DOTA]/\tau} \quad (3)$$

By definition, PRE_{amp} describes the variation of the I/I_0 ratios when the concentration of the paramagnetic agent is zero and approaches infinity:

$$PRE_{amp} = \left(\frac{I}{I_0}\right)_{[Gd-DOTA]=0} - \lim_{[Gd-DOTA]\to\infty}\left(\frac{I}{I_0}\right) \quad (4)$$

Since peak intensities in the NMR spectra were normalized according to Equation (5), Equation (6) can be derived thereof::

$$\left(\frac{I}{I_0}\right)_{[Gd-DOTA]=0} = \left(\frac{I}{I_0}\right) = 1 \quad (5)$$

$$PRE_{amp} = 1 - \lim_{[Gd-DOTA]\to\infty}\left(\frac{I}{I_0}\right) \quad (6)$$

Rearranging this last expression for

$$\lim_{[Gd-DOTA]\to\infty}\left(\frac{I}{I_0}\right) \quad (7)$$

and substituting it into the general form of the exponential decay shown above yields Equation (1) in the main text.

Acknowledgements

This work was supported by NIH grants HL103526 and GM116898 to J.J.C.

Keywords: bicelles · membrane proteins · NMR spectroscopy · paramagnetic relaxation enhancement · transmembrane partition

[1] a) N. F. Endres, R. Das, A. W. Smith, A. Arkhipov, E. Kovacs, Y. Huang, J. G. Pelton, Y. Shan, D. E. Shaw, D. E. Wemmer, J. T. Groves, J. Kuriyan, *Cell*

2013, *152*, 543 – 556; b) L. Z. Mi, C. Lu, Z. Li, N. Nishida, T. Walz, T. A. Springer, *Nat. Struct. Mol. Biol.* **2011**, *18*, 984 – 989; c) Q. Fu, T. M. Fu, A. C. Cruz, P. Sengupta, S. K. Thomas, S. Wang, R. M. Siegel, H. Wu, J. J. Chou, *Mol. Cell* **2016**, *61*, 602 – 613; d) C. Kim, T. Schmidt, E. G. Cho, F. Ye, T. S. Ulmer, M. H. Ginsberg, *Nature* **2011**, *481*, 209 – 213.

[2] a) R. Trenker, M. E. Call, M. J. Call, *J. Am. Chem. Soc.* **2015**, *137*, 15676 – 15679; b) K. Knoblich, S. Park, M. Lutfi, L. van 't Hag, C. E. Conn, S. A. Seabrook, J. Newman, P. E. Czabotar, W. Im, M. E. Call, M. J. Call, *Cell Rep.* **2015**, *11*, 1184 – 1192.

[3] a) M. E. Call, J. J. Chou, *Structure* **2010**, *18*, 1559 – 1569; b) K. R. MacKenzie, J. H. Prestegard, D. M. Engelman, *Science* **1997**, *276*, 131 – 133; c) X. Han, J. H. Bushweller, D. S. Cafiso, L. K. Tamm, *Nat. Struct. Biol.* **2001**, *8*, 715 – 720; d) J. L. Lorieau, J. M. Louis, A. Bax, *Proc. Natl. Acad. Sci. USA* **2010**, *107*, 11341 – 11346; e) M. E. Call, K. W. Wucherpfennig, J. J. Chou, *Nat. Immunol.* **2010**, *11*, 1023 – 1029; f) T. L. Lau, C. Kim, M. H. Ginsberg, T. S. Ulmer, *EMBO J.* **2009**, *28*, 1351 – 1361.

[4] a) C. R. Sanders 2nd, J. P. Schwonek, *Biochemistry* **1992**, *31*, 8898 – 8905; b) C. R. Sanders, B. J. Hare, K. P. Howard, J. H. Prestegard, *Prog. Nucl. Magn. Reson. Spectrosc.* **1994**, *26*, 421 – 444.

[5] C. R. Sanders, R. S. Prosser, *Structure* **1998**, *6*, 1227 – 1234.

[6] Z. Lu, W. D. Van Horn, J. Chen, S. Mathew, R. Zent, C. R. Sanders, *Mol. Pharmacol.* **2012**, *9*, 752 – 761.

[7] R. R. Vold, R. S. Prosser, *J. Magn. Reson. Ser. B* **1996**, *113*, 267 – 271.

[8] K. J. Glover, J. A. Whiles, G. Wu, N. Yu, R. Deems, J. O. Struppe, R. E. Stark, E. A. Komives, R. R. Vold, *Biophys. J.* **2001**, *81*, 2163 – 2171.

[9] a) E. V. Bocharov, K. S. Mineev, P. E. Volynsky, Y. S. Ermolyuk, E. N. Tkach, A. G. Sobol, V. V. Chupin, M. P. Kirpichnikov, R. G. Efremov, A. S. Arseniev, *J. Biol. Chem.* **2008**, *283*, 6950 – 6956; b) J. Dev, D. Park, Q. Fu, J. Chen, H. J. Ha, F. Ghantous, T. Herrmann, W. Chang, Z. Liu, G. Frey, M. S. Seaman, B. Chen, J. J. Chou, *Science* **2016**, *353*, 172 – 175; c) E. A. Morrison, G. T. DeKoster, S. Dutta, R. Vafabakhsh, M. W. Clarkson, A. Bahl, D. Kern, T. Ha, K. A. Henzler-Wildman, *Nature* **2011**, *481*, 45 – 50.

[10] H. Wu, S. G. Hymowitz in *Handbook of cell signaling*, Vol. 1, 2nd ed. (Eds.: R. A. Bradshaw, E. A. Dennis), Academic Press, Oxford, **2009**, pp. 265 – 275.

[11] W. S. Son, S. H. Park, H. J. Nothnagel, G. J. Lu, Y. Wang, H. Zhang, G. A. Cook, S. C. Howell, S. J. Opella, *J. Magn. Reson.* **2012**, *214*, 111 – 118.

[12] D. Lee, C. Hilty, G. Wider, K. Wuthrich, *J. Magn. Reson.* **2006**, *178*, 72 – 76.

[13] a) C. Xu, E. Gagnon, M. E. Call, J. R. Schnell, C. D. Schwieters, C. V. Carman, J. J. Chou, K. W. Wucherpfennig, *Cell* **2008**, *135*, 702 – 713; b) C. Fernandez, C. Hilty, G. Wider, K. Wuthrich, *Proc. Natl. Acad. Sci. USA* **2002**, *99*, 13533 – 13537.

[14] a) M. Respondek, T. Madl, C. Gobl, R. Golser, K. Zangger, *J. Am. Chem. Soc.* **2007**, *129*, 5228 – 5234; b) C. Hilty, G. Wider, C. Fernandez, K. Wuthrich, *ChemBioChem* **2004**, *5*, 467 – 473; c) P. Teriete, C. M. Franzin, J. Choi, F. M. Marassi, *Biochemistry* **2007**, *46*, 6774 – 6783; d) M. S. Al-Abdul-Wahid, R. Verardi, G. Veglia, R. S. Prosser, *J. Biomol. NMR* **2011**, *51*, 173 – 183.

[15] a) G. Hernández, C. L. Teng, R. G. Bryant, D. M. LeMaster, *J. Am. Chem. Soc.* **2002**, *124*, 4463 – 4472; b) G. Pintacuda, G. Otting, *J. Am. Chem. Soc.* **2002**, *124*, 372 – 373.

[16] D. Marsh, *Proc. Natl. Acad. Sci. USA* **2001**, *98*, 7777 – 7782.

[17] N. Kučerka, M. P. Nieh, J. Katsaras, *Biochim. Biophys. Acta Biomembr.* **2011**, *1808*, 2761 – 2771.

[18] J. Pencer, M. P. Nieh, T. A. Harroun, S. Krueger, C. Adams, J. Katsaras, *Biochim. Biophys. Acta* **2005**, *1720*, 84 – 91.

[19] K. S. Mineev, K. D. Nadezhdin, S. A. Goncharuk, A. S. Arseniev, *Langmuir* **2016**, *32*, 6624 – 6637.

[20] E. L. Ulrich, H. Akutsu, J. F. Doreleijers, Y. Harano, Y. E. Ioannidis, J. Lin, M. Livny, S. Mading, D. Maziuk, Z. Miller, E. Nakatani, C. F. Schulte, D. E. Tolmie, R. Kent Wenger, H. Yao, J. L. Markley, *Nucl. Acids Res.* **2007**, *36*, D402 – 408.

[21] F. Delaglio, S. Grzesiek, G. W. Vuister, G. Zhu, J. Pfeifer, A. Bax, *J. Biomol. NMR* **1995**, *6*, 277 – 293.

Manuscript received: September 6, 2016
Accepted Article published: October 17, 2016
Final Article published: December 22, 2016